Title

Malaria parasite infection compromises colonization resistance to an enteric pathogen by reducing gastric acidity

Journal

Science Advances, 7(27)

ISSN

2375-2548

Authors

Walker, Gregory T
Yang, Guiyan
Tsai, Julia Y
et al.

Publication Date

2021-07-02

DOI

10.1126/sciadv.abd6232

Peer reviewed

MICROBIOLOGY

Malaria parasite infection compromises colonization resistance to an enteric pathogen by reducing gastric acidity

Gregory T. Walker[1], Guiyan Yang[1,2], Julia Y. Tsai[1,3], Jorge L. Rodriguez[1], Bevin C. English[1], Franziska Faber[1,4], Lattha Souvannaseng[1,5,6], Brian P. Butler[6], Renée M. Tsolis[1]*

Malaria parasite infection weakens colonization resistance against *Salmonella enterica* serovar (*S.*) Typhimurium. *S.* Typhimurium is a member of the Enterobacterales, a taxon that increases in abundance when the colonic microbiota is disrupted or when the colonic mucosa is inflamed. However, here, we show that infection of mice with *Plasmodium yoelii* enhances *S.* Typhimurium colonization by weakening host control in the upper GI tract. *P. yoelii*–infected mice had elevated gastric pH. Stimulation of gastric acid secretion during *P. yoelii* infection restored stomach acidity and colonization resistance, demonstrating that parasite-induced hypochlorhydria increases gastric survival of *S.* Typhimurium. Furthermore, blockade of *P. yoelii*–induced TNF-α signaling was sufficient to prevent elevation of gastric pH and enhance *S.* Typhimurium colonization during concurrent infection. Collectively, these data suggest that abundance in the fecal microbiota of facultative anaerobes, such as *S.* Typhimurium, can be increased by suppressing antibacterial defenses in the upper GI tract, such as gastric acid.

INTRODUCTION

Facultative anaerobic bacteria of the order Enterobacterales (*1*) are minority species commonly present in the fecal microbiota of healthy adults (*2*). An expansion of this taxon in the fecal microbiota is a signature of dysbiosis (*3*), which is associated with a disruption of the colonic microbiota by antibiotics (*4*) or linked to inflammation of the colon in patients with ulcerative colitis (*5*) or colorectal cancer (*6*). Pathogenic members of the Enterobacterales, such as *Salmonella enterica* serovar (*S.*) Typhimurium, *Citrobacter rodentium*, or *Yersinia enterocolitica*, use their virulence factors to trigger colitis, thereby altering the intestinal environment to increase the availability of respiratory electron acceptors, which fuel pathogen growth to escalate fecal shedding (*7*–*11*). Infection of mice with the parasite *Toxoplasma gondii* triggers intestinal inflammation and bacterial dysbiosis characterized by an expansion of commensal Enterobacterales in the fecal microbiota (*12*, *13*). *T. gondii* infection induces a dysbiosis dominated by Enterobacterales by triggering an influx of macrophages, which produce nitric oxide that is converted in the gut lumen into nitrate, thereby fueling growth of commensal Enterobacterales through nitrate respiration (*14*).

We recently reported that infection with a malaria parasite, *Plasmodium yoelii*, increases the abundance of *S.* Typhimurium in the fecal microbiota of mice (*15*), which might contribute to the increased risk of malaria patients to develop invasive bloodstream infections with nontyphoidal *Salmonella* (NTS) serotypes, such as serovar (*S.*) Typhimurium (*16*, *17*). Infection of mice with *P. yoelii* triggers expression of inflammatory cytokines and inflammatory infiltrates of macrophages and T cells in the cecal mucosa (*15*), but it remains unknown whether parasite-induced intestinal inflammation is responsible for increasing fecal shedding of *S.* Typhimurium during coinfection. Here, we used a coinfection model to interrogate potential interactions by which malaria increases susceptibility to intestinal colonization by *Salmonella*.

RESULTS

P. yoelii infection increases intestinal colonization of *S.* Typhimurium

In experimental malaria models such as *P. yoelii nigeriensis* (henceforth referred to as *P. yoelii*), infection of mice can alter the gut environment (*15*, *18*) and reduce colonization resistance against *S.* Typhimurium (*15*, *19*). However, at later time points after infection, *S.* Typhimurium can overcome colonization resistance because its virulence factors, two type III secretion systems (T3SS-1 and T3SS-2), trigger intestinal inflammation (*9*). To disentangle the contribution of concurrent malaria from the contribution of *S.* Typhimurium virulence factors to weakening colonization resistance, groups of mice were infected with the *S.* Typhimurium wild type or an *invA spiB* mutant that lacks T3SS-1 (due to a mutation in *invA*) and T3SS-2 (due to a mutation in *spiB*) at various time points following *P. yoelii* inoculation (outlined in Fig. 1A). When challenged at 6 days post–*P. yoelii* injection (dpp) or later, a *S.* Typhimurium *invA spiB* colonized the ceca and colons of *P. yoelii*–infected mice at 10- to 100-fold higher levels than in control mice (Fig. 1, B and C, and fig. S1A). This was independent of *S.* Typhimurium virulence, as both wild-type and the *invA spiB* mutant displayed enhanced colonization (fig. S1B). The 6-dpp time point correlated with a peak in parasite expansion in the blood (fig. S2A). By this time, mice infected with *P. yoelii* had consistently developed severe anemia (fig. S2B) and showed substantial weight loss (fig. S2C), while splenomegaly increased steadily throughout the parasite infection (fig. S2D). Therefore, 6 days following *P. yoelii* inoculation was determined to be the earliest reliable time point to interrogate underlying causes of the malaria-associated

[1]Department of Medical Microbiology and Immunology, School of Medicine, University of California Davis, Davis, CA, USA. [2]College of Veterinary Medicine, China Agricultural University, Beijing 100193, China. [3]School of Veterinary Medicine, University of California Davis, Davis, CA, USA. [4]Institute for Molecular Infection Biology (IMIB), Faculty of Medicine, University of Würzburg, D-97080 Würzburg, Germany. [5]Mouse Biology Program, University of California Davis, Davis, CA, USA. [6]Department of Pathobiology, School of Veterinary Medicine, St. George's University, Grenada, West Indies.
*Corresponding author. Email: rmtsolis@ucdavis.edu

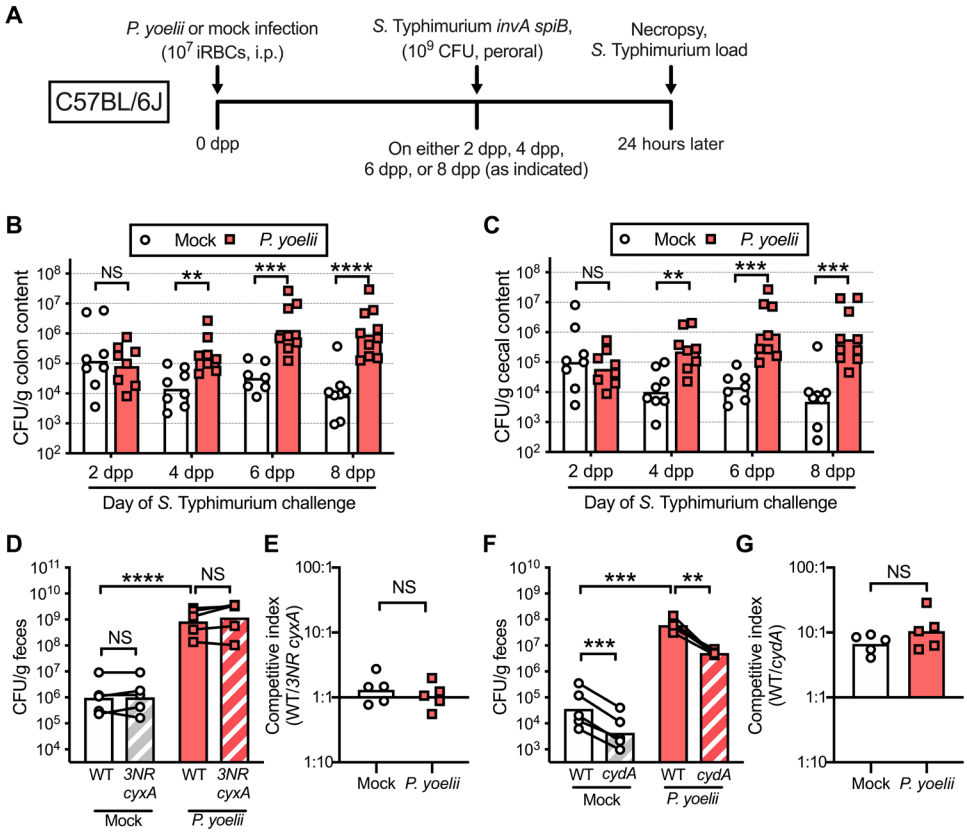

Fig. 1. Enhanced colonization by *S.* Typhimurium in *P. yoelii*–infected mice is independent of nitrate and oxygen respiratory growth by *Salmonella*. (**A**) Schematic outlining the coinfection model used in (**B**) and (**C**). *P. yoelii*– and mock-infected mice were challenged at 2, 4, 6, or 8 days after infection (as indicated) with 10^9 CFU *Salmonella* Typhimurium *invA spiB* Kan^R (peroral). i.p., intraperitoneal. *Salmonella* loads in the colon (B) and cecum (C) were determined 24 hours after *Salmonella* infection. Data are pooled from two separate experiments with three to six mice per time point ($n = 7$ to 10 total per group). (**D** to **G**) Mock- and *P. yoelii*–inoculated mice ($n = 5$ per group) were gavaged at 6 dpp with approximately 5×10^8 CFU wild-type *S.* Typhimurium (WT) and 5×10^8 CFU of either a *S.* Typhimurium *napA narZ narG cyxA* mutant (*3NR cyxA*, D and E) or a *S.* Typhimurium *cydA* mutant (F and G). (D) Fecal *S.* Typhimurium CFUs and (E) competitive indices (WT/*3NR cyxA*) at 24 hpi. (F) Fecal *S.* Typhimurium CFUs and (G) competitive indices (WT/*cydA*) at 24 hpi. Bars represent the geometric mean. Each symbol or linked pair of symbols represents data from one animal. $^{**}P \leq 0.01$, $^{***}P \leq 0.001$, and $^{****}P \leq 0.0001$. NS, not significant.

defect in colonization resistance and was used as the primary model in subsequent experiments.

Impact of nitrate- and oxygen-associated growth on boosting *S.* Typhimurium colonization

Because macrophages recruited during *T. gondii* parasite infection fuel growth of commensal Enterobacterales through nitrate respiration (*14*) and previous work shows that *P. yoelii* infection also recruits macrophages to the cecal mucosa (*15*), we hypothesized that concurrent malaria might increase the luminal availability of nitrate to fuel a *S.* Typhimurium expansion. To test this idea, we compared the fitness of the *S.* Typhimurium wild type with a mutant lacking nitrate reductase activity (*napA narG narZ cyxA* mutant) by infecting mice with a 1:1 mixture of both strains. Genetic ablation of nitrate respiration did not reduce the fitness of *S.* Typhimurium in *P. yoelii*–infected mice (Fig. 1, D and E), despite increased intestinal burden overall in the coinfected group. This finding indicated that nitrate utilization was dispensable for increased fecal recovery of *S.* Typhimurium during concurrent malaria.

Alternatively, it has been shown that inflammation also benefits *S.* Typhimurium via increasing the bioavailability of oxygen. Depletion of *Clostridia*, either through *S.* Typhimurium virulence-associated inflammation or antibiotic administration, results in decreased microbiota production of the short-chain fatty acid (SCFA) butyrate, which typically fuels epithelial colonocytes responsible for maintaining luminal hypoxia (*9*). Reduced butyrate availability switches colonocyte primary metabolism away from oxygen-intensive breakdown of SCFAs, allowing increased diffusion of oxygen into the colonic lumen. This provides an additional respiratory electron acceptor for growth of facultative anaerobes such as *Salmonella* and *E. coli* using cytochrome oxidases (*9*, *20*, *21*). As our previous work found that *P. yoelii* infection can affect the microbiota, including a relative reduction in *Clostridia* in the feces (*15*), we hypothesized this could be opening the oxygen respiratory niche in the colon and promoting *Salmonella* growth. To test this idea, we compared the fitness of the *S.* Typhimurium wild type with a mutant lacking the high-affinity cytochrome *bd* oxidase (*cydA* mutant). However, although *cydA* provided an approximately 10-fold fitness advantage in *P. yoelii*–infected mice, a similar fitness advantage was observed in mice not exposed to *P. yoelii* (Fig. 1, F and G), suggesting that increased oxygenation of the intestinal lumen in coinfected mice did not contribute to the heightened *S.* Typhimurium levels. Overall, these results

indicate that increased access to respiratory electron acceptors was not a major contributing factor to the defect in colonization resistance during *P. yoelii* infection.

P. yoelii infection does not rapidly increase intestinal *S.* Typhimurium replication

The absence of *Plasmodium*-enhanced respiratory growth defects led us to question whether reduced colonization resistance was actually coupled with more rapid growth of *S.* Typhimurium in coinfected mice. To evaluate this, mice were inoculated with *S.* Typhimurium carrying the lactose-addicted plasmid pAM34 (*22*), which allows for the short-term assessment of bacterial growth in low-lactose environments such as the adult mouse intestine (*23*). At 24 hours after challenge, *S.* Typhimurium populations throughout the gut exhibited equivalent replication rates in both *P. yoelii* coinfected and mock-infected mice, despite increased bacterial burdens in the coinfected group (Fig. 2, A and B). Intriguingly, we found that *S.* Typhimurium colonization was already greater in coinfected mice by 4 hours after challenge, also independent of the in vivo growth rate (Fig. 2, C and D). This rapid difference in *S.* Typhimurium loads without a concomitant increase in replication indicated that boosted growth of the bacteria is not responsible for the enhanced colonization of *P. yoelii*–infected mice.

P. yoelii infection affects gastric antibacterial defense

Because differences in *S.* Typhimurium loads arose rapidly after bacterial inoculation of mice, we hypothesized that *P. yoelii* infection

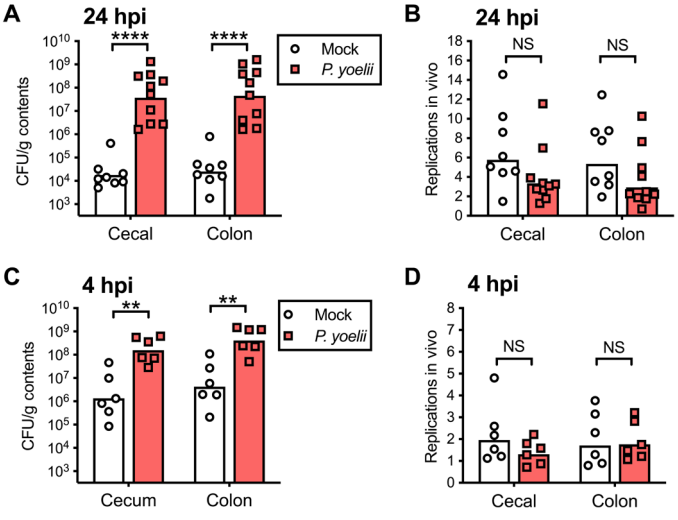

Fig. 2. *S.* Typhimurium intestinal burden is higher in *Plasmodium* coinfected mice despite equivalent bacterial growth. Mice infected with *P. yoelii* (red squares) or mock-infected (white circles) were challenged at 6 dpp with and oral dose of 10^9 CFU *S.* Typhimurium *invA spiB* Cm^R + pAM34 for assessment of the in vivo replication rate of the pathogen. (**A**) *S.* Typhimurium load in the cecal and colon contents 24 hours after inoculation. (**B**) Generation of the *S.* Typhimurium population based on pAM34 plasmid retention quantified 24 hours after inoculation. (**C**) *S.* Typhimurium load in the cecal and colon contents 4 hours after inoculation. (**D**) Generation of the *S.* Typhimurium population based on pAM34 plasmid retention quantified 4 hours after inoculation. Data in (A) and (B) are pooled from two separate experiments for a total of $n = 8$ mice in the mock group and $n = 10$ total mice in the *P. yoelii*–infected group. Data in (C) and (D) represent a single experiment with $n = 6$ mice per group. Each symbol represents data from one animal. Bars represent the geometric mean. $^{**}P \leq 0.01$ and $^{****}P \leq 0.0001$.

may compromise intrinsic "bottleneck" defenses against bacterial colonization that act early following pathogen ingestion. As we also observed that coinfected mice often exhibited higher *S.* Typhimurium levels throughout the upper gastrointestinal (GI) tract (fig. S3A), it seemed likely that loss of colonization resistance against *S.* Typhimurium in coinfected mice could be occurring in the stomach or small intestine.

One of the most severe initial bottlenecks against colonization by many enteric pathogens is imposed by the highly acidic (pH 1.5 to 3) environment encountered in the stomach (*24*). While *S.* Typhimurium thrives at neutral pH (*25*), it is capable of surviving short-term (60 min) exposure to acidity as low as pH 4 in vitro (Fig. 3A). However, inoculated bacteria are rapidly killed at pH 3.5 or lower, with no bacteria recovered from exposure to media at pH 2.5 or below (Fig. 3A). A similar degree of acid sensitivity is shared by many Enterobacterales, including both pathogenic and nonpathogenic varieties (fig. S4, A to E). This finding corroborates previous work indicating that *S.* Typhimurium and other enteric pathogens are highly susceptible to killing by the acid levels present in the stomach (*24*). Thus, deficiencies in maintaining gastric acidity could result in greater survival of ingested *S.* Typhimurium into the intestines.

When measuring the acidity of the stomach lumen directly using a pH-sensing microelectrode, *P. yoelii* infection was associated with a significantly higher gastric pH (mean pH = 4.02 ± 1.07) compared to mock-infected mice (mean pH = 2.46 ± 0.32) by 6 dpp (Fig. 3B). Onset of hypochlorhydria during *P. yoelii* infection correlated with the loss of colonization resistance, as it was not detectable in mice earlier than 6 dpp (fig. S3B). Stomachs of mice at 6 dpp were generally smaller than mock-infected controls (fig. S5A), likely resulting in part from reduced food consumption (fig. S5B) that paralleled observed weight loss patterns during parasite infection (fig. S2C). As meal intake can be stimulatory for gastric acid secretion (*26*), we predicted that the observed pH differences were a result of acute reductions in food intake during malaria. Fasting mock-infected mice overnight was sufficient to reduce stomach weight (fig. S5C) but did not alter the gastric pH of the fasted mice compared to fed mice with ad libitum food access (fig. S5D). Fasting also did not normalize colonization resistance against inoculated *S.* Typhimurium between fasted mock- and *P. yoelii*–infected mice (fig. S5E), suggesting that more than acute decreases in food intake during *P. yoelii* infection is necessary to explain the defects in gastric acidity and susceptibility to *S.* Typhimurium colonization.

Malaria-induced reduction in gastric acidity affects *S.* Typhimurium colonization

We next wanted to determine whether the observed hypochlorhydria is actually responsible for the increased survival of coinfected *S.* Typhimurium. Gastric acid secretion is normally regulated through a combination of stimulatory and inhibitory signaling to gastric parietal cells, leading to translocation of the gastric proton pump to the apical membrane and active acid secretion into gastric lumen (*26*). One of the most potent prosecretion signals is histamine, released locally by enterochromaffin-like cells in the gastric glands, binding parietal cell H2 receptors (H2R) (*26*). To assess whether the high gastric pH during *P. yoelii* infection was responsible for the defect in colonization resistance, mice were treated with the specific H2R agonist dimaprit dihydrochloride to stimulate gastric acid secretion 1 hour before *S.* Typhimurium challenge. H2R agonist administration acutely reduced the stomach pH in *P. yoelii*–infected animals to mock-infected levels (Fig. 3C). Furthermore, H2R stimulation

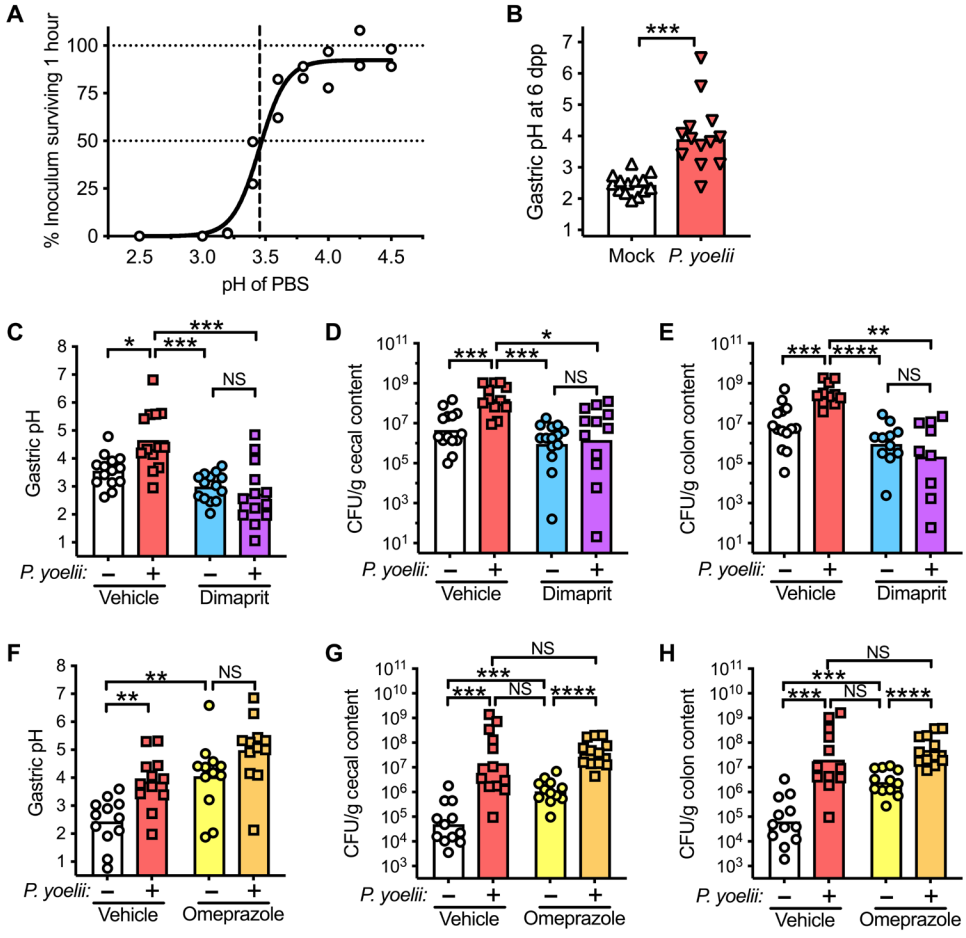

Fig. 3. *P. yoelii*–infected mice develop hypochlorhydria that affects colonization of *S.* Typhimurium. (**A**) *S.* Typhimurium survival in PBS at various pHs. Circles represent individual replicates while the curve is the nonlinear regression (4PL). Horizontal lines indicate 100 and 50 percent survival, while the vertical line marks the pH associated with 50 percent survival. (**B**) Gastric pH of mice 6 days after *P. yoelii* or mock infection. (**C** to **E**) The stomach pH (C), cecal (D) and colon (E) *S.* Typhimurium loads of *P. yoelii*– and mock-infected mice treated with Dimaprit or vehicle on 6 dpp, then challenged with *S.* Typhimurium *invA spiB* Kan^R (peroral) for 4 hours. (**F** to **H**) The stomach pH (F), cecal (G), and colon (H) *S.* Typhimurium loads of mock- and *P. yoelii*–infected mice treated with Omeprazole or vehicle on 3, 4, and 5 dpp and challenged on 6 dpp with *S.* Typhimurium *invA spiB* Kan^R (peroral) for 24 hours. (C to H) Combined data from separate experiments with $n = 6$ to 8 mice per group. Bars represent the geometric mean, and symbols represent data from individual mice. *$P \leq 0.05$, **$P \leq 0.01$, ***$P \leq 0.001$, and ****$P \leq 0.0001$.

in *P. yoelii*–infected mice rescued colonization resistance against *S.* Typhimurium (Fig. 3, D and E) without affecting other aspects of the parasite infection, including parasitemia (fig. S6A) and anemia (fig. S6B).

In complementary experiments, mice were treated with the proton pump inhibitor omeprazole to block acid secretion into the stomach lumen before *S.* Typhimurium challenge. Omeprazole treatment in control mice resulted in a rise in both the gastric pH (Fig. 3F) and *S.* Typhimurium burden (Fig. 3, G and H) relative to vehicle-treated mice, as has been previously observed (*24*). However, omeprazole administration in *P. yoelii*–infected animals did not further increase *S.* Typhimurium loads over *P. yoelii*–infected mice given the vehicle (Fig. 3, G and H) and had no impact on measures of parasite infection severity (fig. S6, C and D). This suggests that the effect of *P. yoelii* infection alone on stomach pH was sufficient to maximally benefit inoculated bacteria in better surviving the gastric environment. Collectively, these data indicate that reduced gastric acidity in *P. yoelii*–infected mice contributes to their increased susceptibility to *S.* Typhimurium infection, as the parasite-associated hypochlorhydria is necessary for boosted survival of inoculated bacteria in the stomach, which, in turn, promotes intestinal colonization.

Altered expression of gastric signaling peptides during malaria

To explore potential mechanisms underlying the rise in gastric pH, we analyzed the effect of *P. yoelii* on the expression of genes associated with regulation of acid secretion by parietal cells in the stomach (*26*). Notably, in the stomach tissues of *P. yoelii*–infected mice, expression of the parietal-stimulatory hormone gastrin (*Gast*) was reduced two- to fourfold (Fig. 4A), while transcripts for the inhibitory hormone somatostatin (*Sst*) were increased nearly twofold relative to mock (Fig. 4B). This result suggested that alterations in typical signaling mechanisms governing acid secretion could be contributing to hypochlorhydria.

Parietal cells use specialized H^+- and K^+-dependent adenosine triphosphatases (H^+,K^+-ATPases; ATP4) concentrated intracellularly on tubulovesicles that localize apically when stimulated to actively secrete protons into the stomach lumen, generating the low pH (*26*, *27*).

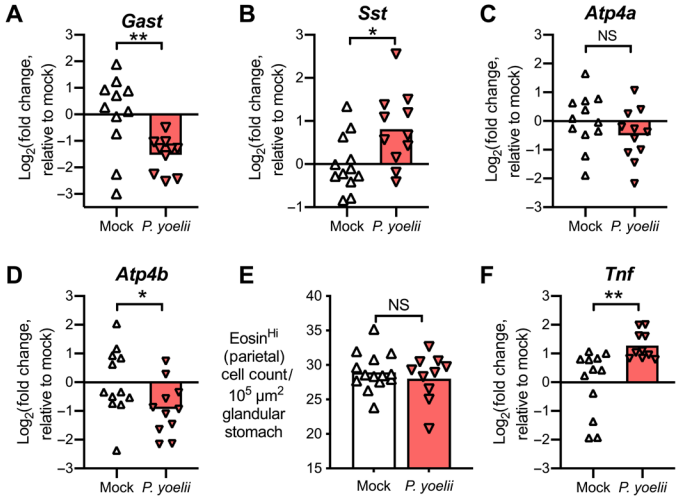

Fig. 4. *P. yoelii* alters stomach expression of acid secretion and inflammatory signals. Relative expression of the mRNA for the gastric signaling peptides gastrin (**A**, *Gast*), somatostatin (**B**, *Sst*), parietal cell proton pump subunits ATP4-α (**C**, *Atp4a*) and ATP4-β (**D**, *Atp4b*), and TNF-α (**F**, *Tnf*) in gastric tissues of mock and *P. yoelii*–infected mice at 6 dpp. Gene expression was quantified relative to β-actin and normalized to average mock-infected levels. (**E**) Quantification of highly eosinophilic cells in H&E-stained gastric tissue sections from mock- and *P. yoelii*–infected mice at 6 dpp. Bars represent the mean. $^*P \leq 0.05$ and $^{**}P \leq 0.01$.

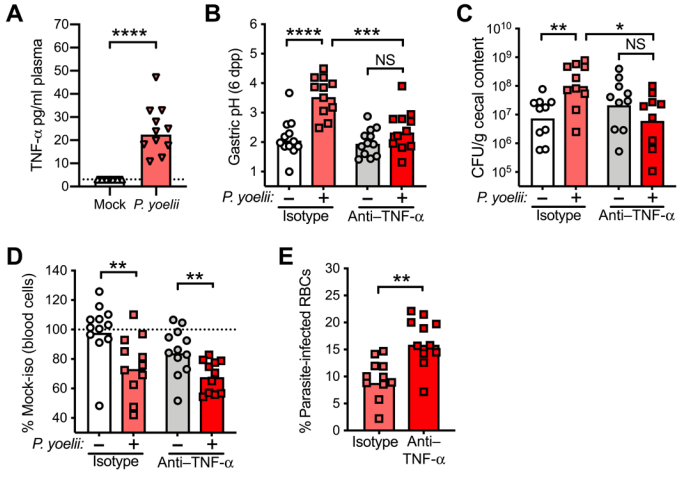

Fig. 5. TNF-α responses to *P. yoelii* infection induce hypochlorhydria and promote *S.* Typhimurium colonization. (**A**) Circulating TNF-α levels detected in plasma at 6 dpp by ELISA in mock-infected or *P. yoelii*–infected mice. Data represent two separate experiments with $n = 5$ to 6 mice in each group. The dotted line represents the limit of detection. (**B** to **E**) On 3 and 5 dpp, mock-infected and *P. yoelii*–infected mice were treated with either anti-mouse TNF-α antibody or an isotype control antibody, and either euthanized at 6 dpp for assessment of the response on measures of parasite infection (B, D, and E) or challenged at 6 dpp with 10^9 CFU *S.* Typhimurium *invA spiB* Kan^R (oral) to quantify the effect of the treatment on *S.* Typhimurium load at 3 hpi (C). Gastric pH (B), cecal *S.* Typhimurium loads (C), relative circulating blood cell counts (D), and parasitemia (E) were determined at necropsy. Data represent three separate experiments with $n = 3$ to 4 mice per group. Bars represent the mean (B) or the geometric mean (A, C, D, and E). $^*P \leq 0.05$, $^{**}P \leq 0.01$, $^{***}P \leq 0.001$, $^{****}P \leq 0.0001$.

Intriguingly, expression of genes encoding the proton pump (*Atp4a/b*) was slightly reduced in the stomach during malaria, with *Atp4b* notably reduced twofold relative to mock mice (Fig. 4, C and D). Gastric acid secretion is not typically regulated by altering the expression of proton pump components, so we explored whether this reduction in transcript abundance instead paralleled a reduction in parietal cell abundance, the primary cells expressing *Atp4a/b*. Blinded histopathology of hematoxylin and eosin (H&E)–stained gastric tissues was imaged by light microscopy (fig. S7A) and fluorescence imaging (fig. S7B) to more accurately quantify highly eosinophilic cells. Eosin is autofluorescent and parietal cells stain strongly with eosin compared to other cell populations in the gastric mucosa; thus, large autofluorescent cells in H&E-stained gastric tissue sections are mostly parietal cells (*28*). We compared eosin-stained cell counts between mock and *P. yoelii*–infected animals in the gastric tissues as a proxy to estimate parietal cell abundance (workflow provided in fig. S7C). However, this analysis found no discernable difference in the overall parietal cell abundance in gastric tissues during malaria (Fig. 4E), suggesting that elevated pH may result from reduced mRNA abundance of genes encoding the proton pump in the stomachs of *Plasmodium*-infected animals.

Proinflammatory signaling during malaria reduces gastric acidity

We next investigated how the immune response to *P. yoelii* may be affecting gastric acid production. In the course of assessing gastric gene expression, we observed elevated transcripts for the inflammatory cytokine tumor necrosis factor–α (TNF-α, encoded by *Tnf*) in the stomach tissue of *P. yoelii*–infected mice (Fig. 4F). TNF-α treatment was reported to reduce secretagogue responses by rabbit parietal cells (*29*), and TNF-α administration induced apoptosis of rat parietal cells (*30*). Moreover, it is known that both clinical and experimental malaria can be associated with elevated circulating TNF-α (*31*–*33*), a response that is thought to help control parasite replication (*31*, *34*) but can also be associated with severe or cerebral malaria (*32*, *33*, *35*). In line with these findings, circulating TNF-α was also higher with *P. yoelii* infection than in control mice (Fig. 5A). Thus, we hypothesized that TNF-α responses to the parasite might be interfering with gastric acid secretion.

In mice treated with TNF-α neutralizing antibody, mock- and *P. yoelii*–infected groups displayed equivalent gastric pH (Fig. 5B and fig. S8A), suggesting that TNF-α signaling is necessary for development of hypochlorhydria with *P. yoelii*. In the context of *S.* Typhimurium, TNF-α blockade also equalized initial [3 hours postinfection (hpi)] colonization between mock- and *P. yoelii*–infected mice (Fig. 5C and fig. S8B), compared to groups treated with an isotype control. Longer challenge time points were not assessed, as TNF-α responses are also necessary for appropriate host defenses to limit systemic *S.* Typhimurium infection (*36*, *37*). Despite TNF-α blockade, mice infected with *Plasmodium* still developed anemia (Fig. 5D) and displayed even greater circulating parasitemia (Fig. 5E). This latter impact on parasite burden is actually evidence of effective antibody blockade, as early TNF-α responses to *Plasmodium* are associated with limiting parasite replication in the host (*34*, *35*). TNF-α blockade did not significantly affect food consumption or weight loss in infected mice, compared with isotype-treated controls (fig. S8, C to E). *P. yoelii*–infected mice given anti–TNF-α antibody still showed an increase in gastric TNF-α transcripts (fig. S8F), but TNF-α blockade led to a reduction of pro–interleukin-1β expression (fig. S8G), indicating a potential dampening of the proinflammatory cytokine response. Overall, these results link proinflammatory TNF-α

responses by the host during *P. yoelii* infection with loss of the intrinsic gastric acid defense, thereby increasing susceptibility to secondary infection by enteric pathogens.

DISCUSSION

The expansion of facultative anaerobic bacteria in the fecal microbiota has been associated with disruption of the colonic microbiota by antibiotics (*4*) and additionally can occur during inflammation of the colon in patients with ulcerative colitis (*5*) or colorectal cancer (*6*). While in these instances, increase in the relative abundance of facultative anaerobes such as Enterobacterales has been linked to alterations in the colonic environment, our results demonstrate that changes to stomach acid, an antimicrobial defense of the upper GI tract, can affect the composition of the fecal microbiota. Thus, our findings on how malaria affects colonization resistance to *S.* Typhimurium, a foodborne microbe, have implications for understanding factors affecting the composition of the microbiota in the lower GI tract, as assessed by fecal microbiota profiling. For example, abundance of bacteria from the oral cavity in the fecal microbiota has been linked to multiple pathogenic processes throughout the digestive tract. Increased prevalence of oral bacteria such as *Fusobacterium* has been found in the fecal microbiota of patients with systemic inflammation caused by inflammatory bowel disease (*38*), liver cirrhosis (*39*), and HIV infection (*5*). This spread of oral bacteria to other sites in the digestive tract is clinically important, especially because some members of the oral microbiota have been linked to colonic (*40*) and pancreatic cancers (*41*). Notably, patients with both AIDS (*42*) and liver cirrhosis (*43*) exhibit hypochlorhydria, although the underlying mechanisms are unknown. Our results suggest that in addition to lowering the barrier to enteric pathogen colonization, inflammation-induced hypochlorhydria may also contribute to spread of oral microbiota to other sites in the digestive tract. Therefore, interpretation of alterations to the fecal microbiota may need to consider habitat filters in the upper GI tract, such as the acidic barrier of the stomach.

Susceptibility to enteric pathogen infection is regulated by both host- and microbiota-associated defenses. Host physiology and immunity influence the distinct habitats of the GI tract, thereby filtering for the most suitable microbial communities throughout (*21*, *44*). The microbiota then serves, in part, to resist pathogen colonization by training host immunity and preempting access to resource and nutrient niches necessary for potential pathogens to thrive in the gut (*44*–*46*). However, many enteric pathogens have evolved virulence systems to avert microbiota-mediated colonization resistance by engineering different growth niches to bloom in the intestine (*7*, *47*). Such mechanisms still typically require sufficient quantities of the pathogen to reach the lower intestines to trigger a substantial host response to alter the gut environment (*48*, *49*). Given this limitation, intrinsic host defenses that rapidly restrict survival of ingested microbes—particularly in the upper GI tract—are necessary to maintain maximal defense against infection. This type of resistance is largely provided by the innate production and secretion of compounds with antibacterial properties, such as host-derived antimicrobial peptides (*45*), various components of bile (*23*, *45*), and gastric acid (*24*, *50*). It is ultimately the combined gauntlet of antimicrobial defenses and nutrient limitation that must be avoided or averted by pathogens to infect the host and cause disease.

Our prior research showed that mice infected with *Plasmodium*, a pathogen that replicates in the bloodstream during the erythrocytic infection state, display increased susceptibility to colonization by NTS (*15*). The findings presented here advance our understanding of how malaria affects colonization resistance to pathogens by linking the boosted implantation of *Salmonella* to a previously unreported, prolonged reduction in gastric acidity associated with inflammatory signaling during infection with the malarial parasite.

Low stomach pH in healthy animals serves as an important bottleneck in the colonization of many bacterial pathogens (*24*), including *S.* Typhimurium and related bacteria (Fig. 3A and fig. S4, A to E). Drugs affecting gastric acidity in humans, such as proton pump inhibitors, have been noted as risk factors that can both alter the gut microbiome and increase susceptibility to intestinal infection with pathogens including *Salmonella*, *Campylobacter*, and *Clostridioides difficile* (*45*, *51*–*54*). In our model, high stomach pH during malaria was associated with increased *S.* Typhimurium abundance after infection, and exogenous stimulation of gastric acid secretion before *S.* Typhimurium inoculation rapidly restored resistance to colonization, demonstrating that parasite-induced hypochlorhydria was responsible for increased susceptibility to the secondary infection.

Typically, parietal cells in the gastric glands are stimulated by a combination of histamine, gastrin, and acetylcholine released from nearby cells, leading to apical translocation of the parietal's H^+/K^+-ATPase proton pump, thereby allowing active acid secretion into the stomach lumen (*26*). Somatostatin serves as the major hormonal inhibitor of gastric acid secretion via direct action on parietal cells and indirectly through inhibition of histamine release by enterochromaffin-like cells. Supporting the notion that *Plasmodium* infection alters normal signaling for gastric acid release, we found increased somatostatin and reduced gastrin expression in gastric tissues from parasite-infected mice (Fig. 4, A and B), which suggests reduced parietal cell stimulation as a mechanism underlying elevated gastric pH. This mechanism is consistent with our findings that parietal cell abundance was unchanged (Fig. 4E) and that stimulation with an H2R agonist resulted in acid production (Fig. 3D).

In the context of gastric *Helicobacter pylori* infection, local production of proinflammatory cytokines, including TNF-α, can influence and inhibit gastric acid secretion by parietal cells (*26*, *29*, *55*). Our results extend this concept to a parasite infection, as antibody blockade of TNF-α signaling during *Plasmodium* infection was sufficient to maintain normal gastric acidity (Fig. 5B) and colonization resistance (Fig. 5C). TNF-α is known to also be involved in both mouse and human innate immune responses to malaria (*33*, *56*) and appears to contribute to limiting parasite replication in host cells (*34*), supporting our data that indicates mice treated with TNF-α blocking antibody develop higher circulating parasitemia (Fig. 5E). This inflammatory cytokine response may represent a shared mechanism between our model and susceptibility to disseminated salmonellosis associated with human malaria. It remains unclear whether the hypoacidic environment could actually be affecting the rest of the microbiota, either directly or indirectly (e.g., through altered digestion or vitamin availability), to produce the shifts in the microbial community composition observed previously (*15*, *19*), or whether these changes are the result of additional GI impacts of *Plasmodium* infection.

In sub-Saharan Africa, malaria is associated with a higher risk for systemic NTS infections in children (*16*, *17*, *57*). While prior work in mouse models helped illuminate how elements of the immune response to *Plasmodium* can promote systemic infections by *S.* Typhimurium

(*58*, *59*), our current findings suggest the additional mechanism of *Plasmodium*-associated hypochlorhydria by which underlying malaria increases susceptibility to colonization by *S.* Typhimurium. This generalized reduction in initial bacterial killing could particularly benefit the multidrug-resistant ST313 isolates now circulating in Africa, which exhibit genomic degradation and reduced capacity for inflammatory activation (*57*). Induction of inflammation is well recognized as part of the usual NTS strategy for colonizing the host (*7*–*9*, *44*, *47*), but avirulent *S.* Typhimurium incapable of inducing a substantial intestinal inflammatory response displayed equivalent colonization enhancement by *P. yoelii* (fig. S1B). This suggests that in the context of malaria, reduced killing of the bacteria in the stomach and upper intestines could compensate for genetic deficits in NTS pathogenesis identified in the now circulating strains. Moreover, malaria-associated suppression of colonization resistance could help clarify why such apparent deficits are not eliminated by selective pressure in the region, allowing development toward an extraintestinal pathogenic lifestyle and ultimately increasing the odds of the high-risk bloodstream NTS infections.

MATERIALS AND METHODS

Mice and experimental coinfection model

Female C57BL/6J mice (6 to 8 weeks old; stock no. 000664) were purchased from the Jackson laboratory for infection experiments. For generating *Plasmodium*-parasitized blood stocks, CD-1 mice were purchased from Charles River Laboratory. Mice were housed under specific pathogen-free conditions and used for experiments at 8 to 11 weeks of age. For most experiments, at least five mice were used in each group, with multiple cages of mice (two to five mice per cage) used for each group to limit the possibility of cage effects. All animal experiments were approved by the Institution of Animal Care and Use Committee at the University of California, Davis (UC Davis).

Plasmodium infections

P. yoelii parasite stock was obtained from the Malaria Research and Reference Reagent Resource and was maintained and expanded by passage through CD-1 mice. Blood from multiple CD-1 mice infected with parasite was collected by cardiac puncture, pooled, and mixed 1:2 (v/v) with freezing solution [10% glycerol and 90% Alsever's solution (Sigma-Aldrich)] for storage in liquid nitrogen. For mock infections, blood was collected from uninfected CD-1 mice and similarly preserved.

C57BL/6J mice were infected with *P. yoelii* parasite upon reaching 8 to 11 weeks of age. Parasitized blood stocks were diluted to 1×10^8 parasite-infected red blood cells/ml with 0.9% saline. Mice were then inoculated intraperitoneally with 0.1 ml of diluted parasitized blood. For mock infections, uninfected control blood was diluted with an equivalent volume of saline, and 0.1 ml was injected intraperitoneally into the mice. Parasite infection was tracked through a combination of weight loss, food consumption, blood cell counts, and parasite burden in the blood. Anemia (reduced circulating blood cell counts) and parasite burden were assessed from blood collected from tail snips. For circulating blood cell counts, tail blood was diluted 1:1000 in phosphate-buffered saline (PBS), and cell concentration was assessed using a TC20 Automated Cell Counter (Bio-Rad Laboratories Inc.). Counts were normalized to the average counts from the mock-treated animals collected and measured at the same time. Parasitemia was determined by examination of Giemsa-stained (Harleco) thin blood smears to enumerate the percentage of red blood cells containing detectable *P. yoelii* parasites.

Salmonella strains

A complete list of *Salmonella* strains used in this study can be found in table S1. Unless otherwise indicated, bacteria were routinely grown on lysogeny broth (LB) agar or MacConkey agar plates and cultured aerobically at 37°C in LB supplemented with antibiotics at the following concentrations for selection when appropriate: nalidixic acid (Nal), 0.05 mg/ml; carbenicillin (Carb), 0.1 mg/ml; kanamycin (Kan), 0.1 mg/ml; and chloramphenicol (Cm), 0.03 mg/ml. Construction of most mutant strains used in this study has been described in prior work (*9*, *22*, *60*–*64*). *S.* Typhimurium *invA spiB* Kan^R (FF459, IR715 Δ*invA* Δ*spiB phoN*::KSAC) was generated by P22 transduction of *phoN*::KSAC from IR715 *phoN*::KSAC into IR715 Δ*invA* Δ*spiB* (SPN487), in the manner previously described for the production of *S.* Typhimurium *invA spiB* Cm^R (FF183) (*60*). *S.* Typhimurium *invA spiB* Cm^R + pAM34 (GTW58) was produced by transforming the plasmid pAM34 (*22*) into FF183 by heat shock, and maintained through culturing in LB with carbenicillin and 1 mM isopropyl β-D-1-thiogalactopyranoside (IPTG).

Salmonella infection and colonization readouts

Single colonies of *S.* Typhimurium grown on selective agar plates were inoculated into LB supplemented with the appropriate antibiotics for selection and incubated with shaking (200 rpm) at 37°C for 14 to 18 hours. Cultures were pelleted by centrifugation (10 min, 4000*g*, 4°C) and washed with sterile LB without antibiotics. Pelleted *S.* Typhimurium was resuspended in LB and adjusted to the appropriate bacterial density for infections. For single-strain infections, mice were inoculated orally by a pipette tip with 0.02 ml of *S.* Typhimurium at a density of approximately 5×10^{10} colony forming units (CFU)/ml. This high inoculum dose was used to help limit variability in colonization between mice in the groups and to reduce nondetection of *Salmonella* in some mice that can occur at lower doses for a more accurate comparison of intestinal burden. For competitive infections, the strains were prepared separately, adjusted to 1×10^{10} CFU/ml, then mixed 1:1 (v/v) and inoculated as 0.1 ml by oral gavage. Inocula were serially diluted and plated for CFU to confirm accuracy of the concentration and the input strain ratio for calculations in competitive infections. *S.* Typhimurium inoculations occurred in the morning, between 06:00 and 12:00. Mice were euthanized at the indicated time points or when they became moribund. Mice euthanized early due to health concerns were excluded from analysis.

Intestinal contents (approximately 20 to 100 mg) of euthanized mice were collected from the relevant portions of the intestines into 1 to 2 ml of PBS and homogenized by vortex. Samples were then serially diluted in PBS and plated on appropriate selective agar to assess CFU loads. If no *S.* Typhimurium could be recovered after challenge, then the load was set to the detection limit for statistical comparisons (100 CFU/g intestinal content). In the *S.* Typhimurium challenges lasting 4 hours or less, mice were excluded from the analysis if *S.* Typhimurium could be detected in the small intestine, but no CFUs were detected in the cecal or colon content, indicating that the inoculum had not yet reached the large intestine at the point of collection. In that case, using the detection limit as the CFU load in the cecum or colon for statistical analysis would be inaccurate. In the competitive infections, intestinal content was plated on media selecting for both inoculated strains (LB + naladixic acid) and the

mutant strain alone (LB + chloramphenicol). Wild-type *S.* Typhimurium (IR715) burden was determined by subtraction of the mutant numbers from the overall (LB + nalidixic acid) numbers, and competitive index was calculated as the wild-type:mutant load, corrected for the input ratio of the inoculum.

In vivo pAM34 growth assays

To compare the approximate in vivo rate of *S.* Typhimurium in *P. yoelii*–infected and mock-infected animals, mice were perorally inoculated with 1×10^9 CFU *S.* Typhimurium *invA spiB* Cm^R + pAM34 (GTW58). As has been previously described (*22*), replication of the pAM34 plasmid is under control of the LacI repressor region, which allows it to be replicated and maintained by *Salmonella* when grown in high concentrations of lactose or a lactose analog such as IPTG but cannot replicate and is rapidly lost as the bacteria divide in low-lactose environments such as the adult mouse. Thus, loss of the plasmid at a population level correlates with the overall replication of the bacteria in the low-lactose environment, which allows for assessment of the replication rate (*23*).

To prepare inocula of *S.* Typhimurium *invA spiB* Cm^R + pAM34, single colonies grown on LB supplemented with carbenicillin (0.1 mg/ml) and 1 mM IPTG (for plasmid maintenance) were inoculated into LB broth (supplemented with IPTG alone) and incubated with shaking (200 rpm) at 37°C for 12 hours. Then, the plasmid was diluted to better assess the early replication rate by subculturing the inoculum (1:100) in fresh LB without IPTG and allowed to grow for an additional 3 hours before harvesting the bacteria by centrifugation and infecting the mice perorally, as previously described. Immediately following infection of the mice, the inoculum was serially diluted in PBS and plated on MacConkey and MacConkey + Carb + 1 mM IPTG to quantify the ratio of pAM34-containing *S.* Typhimurium to the total inoculated *S.* Typhimurium count. At 4 or 24 hours after inoculation, mice were euthanized, and intestinal contents were collected and plated on MacConkey to quantify *S.* Typhimurium burden and determine the fraction of the population maintaining pAM34. In parallel to the mouse infections, serial dilutions of the inoculum were cultured in LB for an additional 4 to 24 hours then plated on MacConkey and MacConkey + Carb + IPTG to generate a standard curve correlating population-level pAM34 plasmid loss to number of replications, as has been previously described (*23*).

In vitro pH bacterial survival assays

To assess bacterial sensitivity to low pH, PBS was acidified to different pH levels between 2 and 5 with hydrochloric acid and aliquoted into separate tubes. *S.* Typhimurium *invA spiB* Kan^R and strains of *Escherichia coli* strain Nissle 1917, *E. coli* O157:H7 EDL933 (ATCC 43895), *C. rodentium* DBS100 (ATCC 51459), *Shigella flexneri* M90T (ATCC BAA-2402), and *Y. enterocolitica subsp. enterocolitica* (ATCC 700823) were grown overnight in LB broth and prepared for inoculating mice as described above, except washed and resuspended using PBS instead of LB, to an optical density at 600 nm (OD_{600}) of 1.0, and plated for quantification of initial CFUs. The inoculum was then diluted 1:100 into the different low-pH PBS tubes and incubated at 37°C with shaking for 1 hour. Samples were serially diluted in fresh PBS (pH 7.4) and plated on MacConkey agar to quantify remaining bacterial concentrations.

Gastric pH assessment

Following euthanasia, stomachs of mice were removed from the body cavity. The microelectrode PH-N and reference probes (Unisense) were immediately inserted into the untreated gastric antral lumen for assessment of pH, and measurements on the Unisense Microsensor Multimeter (in millivolts) were recorded and converted to pH values using a standard curve generated from concurrent readings of reference standards at pH 2, 4, and 7. The probes were rinsed with 70% ethanol and distilled water between measurements.

Histamine H2R agonist (dimaprit) administration

Mice were inoculated with *P. yoelii*–infected or control blood as previously described. In the morning of day 6 after infection, mice received a single dose of the histamine H2R agonist dimaprit dihydrochloride (Tocris Bioscience) or a mock treatment with the vehicle. Dimaprit was administered intraperitoneally as 0.1 ml of dimaprit dihydrochloride (40 mg/ml) dissolved in sterile saline, and the vehicle (saline) was administered in an equivalent volume. One hour later, mice were challenged with *S.* Typhimurium for 4 hours and then assessed for gastric pH and intestinal *S.* Typhimurium burden.

Omeprazole administration

Mice were inoculated with *P. yoelii*–infected or control blood as previously described. In the afternoon on days 3, 4, and 5 after infection, mice began receiving daily treatments with either the proton pump inhibitor omeprazole (Sigma-Aldrich) or a mock treatment with the vehicle. Omeprazole was administered intraperitoneally as 0.1 ml of a suspension (30 mg/ml) in 1% Tween 80 (Sigma-Aldrich) in Dulbecco's phosphate-buffered saline (Gibco), and vehicle was administered in an equivalent volume. At 6 dpp, mice were challenged with *S.* Typhimurium for 24 hours and then assessed for gastric pH and intestinal *S.* Typhimurium burden.

Anti–TNF-α antibody administration

Mice were inoculated with *P. yoelii*–infected or control blood as previously described. On days 3 and 5 after infection, mice received a dose of either Ultra-LEAF Purified anti-mouse TNF-α antibody (clone: MP6-XT22, BioLegend Inc.) or Ultra-LEAF Purified Rat IgG1, κ isotype control antibody (BioLegend Inc.). Both antibodies were diluted to 2 mg/ml in dPBS (Gibco) and administered as 0.25 ml per mouse, intraperitoneally, for a dose of 0.5 mg per mouse (approximately 25 mg/kg body weight). At 6 dpp, mice were either euthanized for relevant measurements or challenged with *S.* Typhimurium for 3 hours then euthanized for gastric pH and intestinal *S.* Typhimurium burden.

RNA extraction and real-time PCR expression analyses

Following lumen content removal, tissues were snap-frozen in liquid nitrogen at necropsy and stored at −80°C. RNA was isolated from tissues using TRI Reagent (Molecular Research Center). Briefly, whole tissues were suspended in TRI Reagent and homogenized by glass bead–beating for 1 min then treated with chloroform and centrifuged to separate the phases. The aqueous phase was removed and mixed with 95% ethanol, then applied to a silica membrane column (EconoSpin, Epoch Life Science), and washed with 3 M sodium acetate. The column was treated with PureLink DNase (Invitrogen) to remove genomic DNA contamination and washed twice with 10 mM Hepes in 70% ethanol, and RNA was eluted in RNase-free water for quantification.

For analysis of mRNA expression, 1 μg of total RNA per sample was reverse-transcribed into complementary DNA (cDNA) in a 50 μl of reaction using MultiScribe Reverse Transcriptase (Thermo Fisher

Scientific), and 4 μl of the resulting cDNA was used for each real-time reaction. Real-time polymerase chain reaction (PCR) was performed using SYBR green (Applied Biosystems) on a ViiA 7 Real-Time PCR System (Applied Biosystems) using primers listed in table S2. Data were analyzed using the comparative threshold cycle method in QuantStudio Real-Time PCR System (Applied Biosystems), with target gene expression levels normalized to *Actb* RNA levels in the same sample and represented as fold change over the average expression in mock-infected animals.

Gastric histopathology

At necropsy, stomachs were flayed open along the lesser curvature and samples of the greater curvature approximately 5 mm wide at the midline were collected from the forestomach to pyloric sphincter, as described by Sigal *et al.* (*65*), and embedded in paraffin to generate longitudinal sections. Five-micrometer-thick tissue sections were cut from formalin-fixed paraffin-embedded tissues and H&E-stained by the UC Davis Veterinary Pathology Laboratory. Blinded images of stained slides were taken as both bright-field (20×) and autofluorescence (40×, red fluorescent protein channel; excitation: 531/40, emission: 593/40) scans using an EVOS FL imaging microscope (Thermo Fisher Scientific) for general histopathological assessment and highly eosinophilic (autofluorescent) cell quantification.

To assess eosinophilic cell abundance in the gastric mucosa to estimate parietal cell abundance (*28*), images of glandular/mucosal portions of the tissues distal to the forestomach–corpus junction were bounded manually, and the glandular area was measured using ImageJ. Then, the images were made binary, holes were filled, watershed was used to separate nearby cell structures, and large particles (radius > 25 μm) were analyzed. As this process often grouped multiple, closely associated parietal cells as single particles (see overlay example in fig. S7C, right), analyzed particles were converted to approximate cell numbers by dividing the particle area in each image by the overall median particle size.

Plasma TNF-α measurements

Blood was collected from mice by cardiac puncture using heparinized needles immediately following death by CO_2 inhalation. The heparinized blood was centrifuged (8000*g* for 4 min) and the plasma layer was removed and stored at −80°C for TNF-α measurement using the mouse TNF-α DuoSet ELISA (R&D Systems Inc.) according to the manufacturer's instructions.

Statistical analyses

The investigators were not blinded to animal allocation during experiments and outcome assessment, except for histopathology analysis. Sample sizes were estimated on the basis of effect sizes in previous studies. All analyses were performed using Prism 8 (GraphPad Software, La Jolla, CA). The limit of detection while plating for *S.* Typhimurium loads was set to 100 CFU/g content, and the number of CFU per gram intestinal content was $\log_{10}$-transformed to normalize the data for statistical analysis. Significant differences in $\log_{10}$-normalized CFU loads, gastric pH, and $\log_2$-normalized mRNA expression data between groups were determined by unpaired *t* tests with Welch's correction. Significant differences in CFU loads of competing *S.* Typhimurium strains in the same animal were determined by paired *t* tests. Significant differences between groups in their competitive indices and other measures not log-normalized before comparison (body weight changes, spleen and stomach weights, blood cell counts, parasite burden, and circulating TNF-α) were determined by Mann-Whitney tests. In all comparisons, $P < 0.05$ was considered statistically significant.

Software

The following software were used: Microsoft Excel for Mac, Prism 8 for macOS (GraphPad Software), QuantStudio Real-Time PCR System version 1.3 (Applied Biosystems), EVOS FL Auto 2 Imaging System (Thermo Fisher Scientific), and ImageJ/FIJI version 2.0.0-rc-69/p1.520 (https://imagej.net/Fiji/Downloads) (*66*, *67*).

SUPPLEMENTARY MATERIALS

Supplementary material for this article is available at http://advances.sciencemag.org/cgi/content/full/7/27/eabd6232/DC1

View/request a protocol for this paper from *Bio-protocol*.

REFERENCES AND NOTES

1. M. Adeolu, S. Alnajar, S. Naushad, R. S. Gupta, Genome-based phylogeny and taxonomy of the "*Enterobacteriales*": Proposal for *Enterobacterales* ord. nov. divided into the families *Enterobacteriaceae*, *Erwiniaceae* fam. nov., *Pectobacteriaceae* fam. nov., *Yersiniaceae* fam. nov., *Hafniaceae* fam. nov., *Morganellaceae* fam. nov., and *Budviciaceae* fam. nov. *Int. J. Syst. Evol. Microbiol.* **66**, 5575–5599 (2016).
2. Human Microbiome Project Consortium, Structure, function, and diversity of the healthy human microbiome. *Nature* **486**, 207–214 (2012).
3. N. R. Shin, T. W. Whon, J. W. Bae, Proteobacteria: Microbial signature of dysbiosis in gut microbiota. *Trends Biotechnol.* **33**, 496–503 (2015).
4. E. J. Vollaard, H. A. Clasener, A. J. Janssen, Co-trimoxazole impairs colonization resistance in healthy volunteers. *J. Antimicrob. Chemother.* **30**, 685–691 (1992).
5. S. C. Lee, L. L. Chua, S. H. Yap, T. F. Khang, C. Y. Leng, R. I. Raja Azwa, S. R. Lewin, A. Kamarulzaman, Y. L. Woo, Y. A. L. Lim, P. Loke, R. Rajasuriar, Enrichment of gut-derived *Fusobacterium* is associated with suboptimal immune recovery in HIV-infected individuals. *Sci. Rep.* **8**, 14277 (2018).
6. J. C. Arthur, E. Perez-Chanona, M. Muhlbauer, S. Tomkovich, J. M. Uronis, T. J. Fan, B. J. Campbell, T. Abujamel, B. Dogan, A. B. Rogers, J. M. Rhodes, A. Stintzi, K. W. Simpson, J. J. Hansen, T. O. Keku, A. A. Fodor, C. Jobin, Intestinal inflammation targets cancer-inducing activity of the microbiota. *Science* **338**, 120–123 (2012).
7. S. E. Winter, P. Thiennimitr, M. G. Winter, B. P. Butler, D. L. Huseby, R. W. Crawford, J. M. Russell, C. L. Bevins, L. G. Adams, R. M. Tsolis, J. R. Roth, A. J. Bäumler, Gut inflammation provides a respiratory electron acceptor for *Salmonella*. *Nature* **467**, 426–429 (2010).
8. C. A. Lopez, F. Rivera-Chavez, M. X. Byndloss, A. J. Baumler, The periplasmic nitrate reductase NapABC supports luminal growth of *Salmonella enterica* serovar typhimurium during colitis. *Infect. Immun.* **83**, 3470–3478 (2015).
9. F. Rivera-Chavez, L. F. Zhang, F. Faber, C. A. Lopez, M. X. Byndloss, E. E. Olsan, G. Xu, E. M. Velazquez, C. B. Lebrilla, S. E. Winter, A. J. Bäumler, Depletion of butyrate-producing *Clostridia* from the gut microbiota drives an aerobic luminal expansion of *Salmonella*. *Cell Host Microbe* **19**, 443–454 (2016).
10. K. Kamdar, S. Khakpour, J. Chen, V. Leone, J. Brulc, T. Mangatu, D. A. Antonopoulos, E. B. Chang, S. A. Kahn, B. S. Kirschner, G. Young, R. W. DePaolo, Genetic and metabolic signals during acute enteric bacterial infection alter the microbiota and drive progression to chronic inflammatory disease. *Cell Host Microbe* **19**, 21–31 (2016).
11. C. A. Lopez, B. M. Miller, F. Rivera-Chavez, E. M. Velazquez, M. X. Byndloss, A. Chavez-Arroyo, K. L. Lokken, R. M. Tsolis, S. E. Winter, A. J. Baumler, Virulence factors enhance *Citrobacter rodentium* expansion through aerobic respiration. *Science* **353**, 1249–1253 (2016).
12. M. Raetz, S. H. Hwang, C. L. Wilhelm, D. Kirkland, A. Benson, C. R. Sturge, J. Mirpuri, S. Vaishnava, B. Hou, A. L. Defranco, C. J. Gilpin, L. V. Hooper, F. Yarovinsky, Parasite-induced T_H1 cells and intestinal dysbiosis cooperate in IFN-γ–dependent elimination of Paneth cells. *Nat. Immunol.* **14**, 136–142 (2013).
13. L. M. Haag, A. Fischer, B. Otto, R. Plickert, A. A. Kuhl, U. B. Gobel, S. Bereswill, M. M. Heimesaat, Intestinal microbiota shifts towards elevated commensal *Escherichia coli* loads abrogate colonization resistance against *Campylobacter jejuni* in mice. *PLOS ONE* **7**, e35988 (2012).
14. S. Wang, A. El-Fahmawi, D. A. Christian, Q. Fang, E. Radaelli, L. Chen, M. C. Sullivan, A. M. Misic, J. A. Ellringer, X.-Q. Zhu, S. E. Winter, C. A. Hunter, D. P. Beiting, Infection-induced intestinal dysbiosis is mediated by macrophage activation and nitrate production. *MBio* **10**, e00935-19 (2019).
15. J. P. Mooney, K. L. Lokken, M. X. Byndloss, M. D. George, E. M. Velazquez, F. Faber, B. P. Butler, G. T. Walker, M. M. Ali, R. Potts, C. Tiffany, B. M. Ahmer, S. Luckhart, R. M. Tsolis,

Inflammation-associated alterations to the intestinal microbiota reduce colonization resistance against nontyphoidal *Salmonella* during concurrent malaria parasite infection. *Sci. Rep.* **5**, 14603 (2015).
16. T. T. Ao, N. A. Feasey, M. A. Gordon, K. H. Keddy, F. J. Angulo, J. A. Crump, Global burden of invasive nontyphoidal *Salmonella* disease, 2010(1). *Emerg. Infect. Dis.* **21**, 941–949 (2015).
17. E. N. Takem, A. Roca, A. Cunnington, The association between malaria and nontyphoid *Salmonella* bacteraemia in children in sub-Saharan Africa: A literature review. *Malar. J.* **13**, 400 (2014).
18. J. E. Denny, J. B. Powers, H. F. Castro, J. Zhang, S. Joshi-Barve, S. R. Campagna, N. W. Schmidt, Differential sensitivity to *Plasmodium yoelii* infection in C57BL/6 mice impacts gut-liver axis homeostasis. *Sci. Rep.* **9**, 3472 (2019).
19. T. Taniguchi, E. Miyauchi, S. Nakamura, M. Hirai, K. Suzue, T. Imai, T. Nomura, T. Handa, H. Okada, C. Shimokawa, R. Onishi, A. Olia, J. Hirata, H. Tomita, H. Ohno, T. Horii, H. Hisaeda, *Plasmodium berghei* ANKA causes intestinal malaria associated with dysbiosis. *Sci. Rep.* **5**, 15699 (2015).
20. Y. Litvak, K. K. Z. Mon, H. Nguyen, G. Chanthavixay, M. Liou, E. M. Velazquez, L. Kutter, M. A. Alcantara, M. X. Byndloss, C. R. Tiffany, G. T. Walker, F. Faber, Y. Zhu, D. N. Bronner, A. J. Byndloss, R. M. Tsolis, H. Zhou, A. J. Bäumler, Commensal enterobacteriaceae protect against *Salmonella* colonization through oxygen competition. *Cell Host Microbe* **25**, 128–139.e5 (2019).
21. Y. Litvak, A. J. Baumler, Microbiota-nourishing immunity: A guide to understanding our microbial self. *Immunity* **51**, 214–224 (2019).
22. D. Gil, J. P. Bouche, ColE1-type vectors with fully repressible replication. *Gene* **105**, 17–22 (1991).
23. S. Y. Wotzka, M. Kreuzer, L. Maier, M. Arnoldini, B. D. Nguyen, A. O. Brachmann, D. L. Berthold, M. Zund, A. Hausmann, E. Bakkeren, D. Hoces, E. Gül, M. Beutler, T. Dolowschiak, M. Zimmermann, T. Fuhrer, K. Moor, U. Sauer, A. Typas, J. Piel, M. Diard, A. J. Macpherson, B. Stecher, S. Sunagawa, E. Slack, W. D. Hardt, *Escherichia coli* limits *Salmonella* Typhimurium infections after diet shifts and fat-mediated microbiota perturbation in mice. *Nat. Microbiol.* **4**, 2164–2174 (2019).
24. S. M. Tennant, E. L. Hartland, T. Phumoonna, D. Lyras, J. I. Rood, R. M. Robins-Browne, I. R. van Driel, Influence of gastric acid on susceptibility to infection with ingested bacterial pathogens. *Infect. Immun.* **76**, 639–645 (2008).
25. S. Bearson, B. Bearson, J. W. Foster, Acid stress responses in enterobacteria. *FEMS Microbiol. Lett.* **147**, 173–180 (1997).
26. A. C. Engevik, I. Kaji, J. R. Goldenring, The physiology of the gastric parietal cell. *Physiol. Rev.* **100**, 573–602 (2020).
27. M. L. Schubert, Functional anatomy and physiology of gastric secretion. *Curr. Opin. Gastroenterol.* **31**, 479–485 (2015).
28. C. A. Rubio, M. Owston, A. Orrego, E. J. Dick Jr., A simple method to record parietal cells in the fundic mucosa in baboons. *In Vivo* **24**, 705–707 (2010).
29. I. L. Beales, J. Calam, Interleukin 1β and tumour necrosis factor α inhibit acid secretion in cultured rabbit parietal cells by multiple pathways. *Gut* **42**, 227–234 (1998).
30. B. Neu, A. J. Puschmann, A. Mayerhofer, P. Hutzler, J. Grossmann, F. Lippl, W. Schepp, C. Prinz, TNF-alpha induces apoptosis of parietal cells. *Biochem. Pharmacol.* **65**, 1755–1760 (2003).
31. I. C. Hirako, P. A. Assis, N. S. Hojo-Souza, G. Reed, H. Nakaya, D. T. Golenbock, R. S. Coimbra, R. T. Gazzinelli, Daily rhythms of TNFα expression and food intake regulate synchrony of *Plasmodium* stages with the host circadian cycle. *Cell Host Microbe* **23**, 796–808.e6 (2018).
32. K. E. Lyke, R. Burges, Y. Cissoko, L. Sangare, M. Dao, I. Diarra, A. Kone, R. Harley, C. V. Plowe, O. K. Doumbo, M. B. Sztein, Serum levels of the proinflammatory cytokines interleukin-1 β (IL-1β), IL-6, IL-8, IL-10, tumor necrosis factor α, and IL-12(p70) in Malian children with severe *Plasmodium falciparum* malaria and matched uncomplicated malaria or healthy controls. *Infect. Immun.* **72**, 5630–5637 (2004).
33. W. L. Mandala, C. L. Msefula, E. N. Gondwe, M. T. Drayson, M. E. Molyneux, C. A. MacLennan, Cytokine profiles in Malawian children presenting with uncomplicated malaria, severe malarial anemia, and cerebral malaria. *Clin. Vaccine Immunol.* **24**, e00533-16 (2017).
34. L. N. Cruz, Y. Wu, H. Ulrich, A. G. Craig, C. R. Garcia, Tumor necrosis factor reduces *Plasmodium falciparum* growth and activates calcium signaling in human malaria parasites. *Biochim. Biophys. Acta* **1860**, 1489–1497 (2016).
35. I. Angulo, M. Fresno, Cytokines in the pathogenesis of and protection against malaria. *Clin. Diagn. Lab. Immunol.* **9**, 1145–1152 (2002).
36. P. Everest, M. Roberts, G. Dougan, Susceptibility to *Salmonella* typhimurium infection and effectiveness of vaccination in mice deficient in the tumor necrosis factor α p55 receptor. *Infect. Immun.* **66**, 3355–3364 (1998).
37. A. Vazquez-Torres, G. Fantuzzi, C. K. Edwards III, C. A. Dinarello, F. C. Fang, Defective localization of the NADPH phagocyte oxidase to *Salmonella*-containing phagosomes in tumor necrosis factor p55 receptor–deficient macrophages. *Proc. Natl. Acad. Sci. U.S.A.* **98**, 2561–2565 (2001).
38. D. Gevers, S. Kugathasan, L. A. Denson, Y. Vazquez-Baeza, W. Van Treuren, B. Ren, E. Schwager, D. Knights, S. J. Song, M. Yassour, X. C. Morgan, A. D. Kostic, C. Luo, A. Gonzalez, D. McDonald, Y. Haberman, T. Walters, S. Baker, J. Rosh, M. Stephens, M. Heyman, J. Markowitz, R. Baldassano, A. Griffiths, F. Sylvester, D. Mack, S. Kim, W. Crandall, J. Hyams, C. Huttenhower, R. Knight, R. J. Xavier, The treatment-naive microbiome in new-onset Crohn's disease. *Cell Host Microbe* **15**, 382–392 (2014).
39. N. Qin, F. Yang, A. Li, E. Prifti, Y. Chen, L. Shao, J. Guo, E. Le Chatelier, J. Yao, L. Wu, J. Zhou, S. Ni, L. Liu, N. Pons, J. M. Batto, S. P. Kennedy, P. Leonard, C. Yuan, W. Ding, Y. Chen, X. Hu, B. Zheng, G. Qian, W. Xu, S. D. Ehrlich, S. Zheng, L. Li, Alterations of the human gut microbiome in liver cirrhosis. *Nature* **513**, 59–64 (2014).
40. C. L. Sears, W. S. Garrett, Microbes, microbiota, and colon cancer. *Cell Host Microbe* **15**, 317–328 (2014).
41. R. A. Gaiser, A. Halimi, H. Alkharaan, L. Lu, H. Davanian, K. Healy, L. W. Hugerth, Z. Ateeb, R. Valente, C. Fernandez Moro, M. Del Chiaro, M. Sallberg Chen, Enrichment of oral microbiota in early cystic precursors to invasive pancreatic cancer. *Gut* **68**, 2186–2194 (2019).
42. G. Lake-Bakaar, E. Quadros, S. Beidas, M. Elsakr, W. Tom, D. E. Wilson, H. P. Dincsoy, P. Cohen, E. W. Straus, Gastric secretory failure in patients with the acquired immunodeficiency syndrome (AIDS). *Ann. Intern. Med.* **109**, 502–504 (1988).
43. Y. J. Nam, S. J. Kim, W. C. Shin, J. H. Lee, W. C. Choi, K. Y. Kim, T. H. Han, Gastric pH and *Helicobacter pylori* infection in patients with liver cirrhosis. *Korean J. Hepatol.* **10**, 216–222 (2004).
44. R. M. Tsolis, A. J. Baumler, Gastrointestinal host-pathogen interaction in the age of microbiome research. *Curr. Opin. Microbiol.* **53**, 78–89 (2020).
45. Q. R. Ducarmon, R. D. Zwittink, B. V. H. Hornung, W. van Schaik, V. B. Young, E. J. Kuijper, Gut microbiota and colonization resistance against bacterial enteric infection. *Microbiol. Mol. Biol. Rev.* **83**, e00007-19 (2019).
46. M. Sassone-Corsi, M. Raffatellu, No vacancy: How beneficial microbes cooperate with immunity to provide colonization resistance to pathogens. *J. Immunol.* **194**, 4081–4087 (2015).
47. F. Rivera-Chávez, A. J. Bäumler, The pyromaniac inside you: *Salmonella* metabolism in the host gut. *Annu. Rev. Microbiol.* **69**, 31–48 (2015).
48. M. Bohnhoff, B. L. Drake, C. P. Miller, Effect of streptomycin on susceptibility of intestinal tract to experimental *Salmonella* infection. *Proc. Soc. Exp. Biol. Med.* **86**, 132–137 (1954).
49. E. M. Velazquez, H. Nguyen, K. T. Heasley, C. H. Saechao, L. M. Gil, A. W. L. Rogers, B. M. Miller, M. R. Rolston, C. A. Lopez, Y. Litvak, M. J. Liou, F. Faber, D. N. Bronner, C. R. Tiffany, M. X. Byndloss, A. J. Byndloss, A. J. Baumler, Endogenous Enterobacteriaceae underlie variation in susceptibility to *Salmonella* infection. *Nat. Microbiol.* **4**, 1057–1064 (2019).
50. T. C. Martinsen, K. Bergh, H. L. Waldum, Gastric juice: A barrier against infectious diseases. *Basic Clin. Pharmacol. Toxicol.* **96**, 94–102 (2005).
51. J. Leonard, J. K. Marshall, P. Moayyedi, Systematic review of the risk of enteric infection in patients taking acid suppression. *Am. J. Gastroenterol.* **102**, 2047–2056 (2007).
52. C. Bavishi, H. L. Dupont, Systematic review: The use of proton pump inhibitors and increased susceptibility to enteric infection. *Aliment. Pharmacol. Ther.* **34**, 1269–1281 (2011).
53. F. Imhann, M. J. Bonder, A. Vich Vila, J. Fu, Z. Mujagic, L. Vork, E. F. Tigchelaar, S. A. Jankipersadsing, M. C. Cenit, H. J. Harmsen, G. Dijkstra, L. Franke, R. J. Xavier, D. Jonkers, C. Wijmenga, R. K. Weersma, A. Zhernakova, Proton pump inhibitors affect the gut microbiome. *Gut* **65**, 740–748 (2016).
54. R. A. Hafiz, C. Wong, S. Paynter, M. David, G. Peeters, The risk of community-acquired enteric infection in proton pump inhibitor therapy: Systematic review and meta-analysis. *Ann. Pharmacother.* **52**, 613–622 (2018).
55. I. T. Padol, R. H. Hunt, Effect of T_H1 cytokines on acid secretion in pharmacologically characterised mouse gastric glands. *Gut* **53**, 1075–1081 (2004).
56. K. R. Dobbs, J. N. Crabtree, A. E. Dent, Innate immunity to malaria—The role of monocytes. *Immunol. Rev.* **293**, 8–24 (2020).
57. J. J. Gilchrist, C. A. MacLennan, Invasive nontyphoidal *Salmonella* disease in Africa. *EcoSal Plus* **8**, 10.1128/ecosalplus.ESP-0007-2018, (2019).
58. T. S. Nyirenda, W. L. Mandala, M. A. Gordon, P. Mastroeni, Immunological bases of increased susceptibility to invasive nontyphoidal *Salmonella* infection in children with malaria and anaemia. *Microbes Infect.* **20**, 589–598 (2018).
59. J. P. Mooney, L. J. Galloway, E. M. Riley, Malaria, anemia, and invasive bacterial disease: A neutrophil problem? *J. Leukoc. Biol.* **105**, 645–655 (2019).
60. F. Faber, P. Thiennimitr, L. Spiga, M. X. Byndloss, Y. Litvak, S. Lawhon, H. L. Andrews-Polymenis, S. E. Winter, A. J. Baumler, Respiration of microbiota-derived 1,2-propanediol drives *Salmonella* expansion during colitis. *PLOS Pathog.* **13**, e1006129 (2017).
61. I. Stojiljkovic, A. J. Baumler, F. Heffron, Ethanolamine utilization in *Salmonella* typhimurium: Nucleotide sequence, protein expression, and mutational analysis of the cchA cchB eutE eutJ eutG eutH gene cluster. *J. Bacteriol.* **177**, 1357–1366 (1995).

62. R. A. Kingsley, A. D. Humphries, E. H. Weening, M. R. De Zoete, S. Winter, A. Papaconstantinopoulou, G. Dougan, A. J. Baumler, Molecular and phenotypic analysis of the CS54 island of *Salmonella* enterica serotype typhimurium: Identification of intestinal colonization and persistence determinants. *Infect. Immun.* **71**, 629–640 (2003).
63. F. Rivera-Chavez, S. E. Winter, C. A. Lopez, M. N. Xavier, M. G. Winter, S. P. Nuccio, J. M. Russell, R. C. Laughlin, S. D. Lawhon, T. Sterzenbach, C. L. Bevins, R. M. Tsolis, R. Harshey, L. G. Adams, A. J. Baumler, *Salmonella* uses energy taxis to benefit from intestinal inflammation. *PLOS Pathog.* **9**, e1003267 (2013).
64. F. Faber, L. Tran, M. X. Byndloss, C. A. Lopez, E. M. Velazquez, T. Kerrinnes, S. P. Nuccio, T. Wangdi, O. Fiehn, R. M. Tsolis, A. J. Baumler, Host-mediated sugar oxidation promotes postantibiotic pathogen expansion. *Nature* **534**, 697–699 (2016).
65. M. Sigal, M. E. Rothenberg, C. Y. Logan, J. Y. Lee, R. W. Honaker, R. L. Cooper, B. Passarelli, M. Camorlinga, D. M. Bouley, G. Alvarez, R. Nusse, J. Torres, M. R. Amieva, *Helicobacter pylori* activates and expands Lgr5$^+$ stem cells through direct colonization of the gastric glands. *Gastroenterology* **148**, 1392–1404.e21 (2015).
66. J. Schindelin, I. Arganda-Carreras, E. Frise, V. Kaynig, M. Longair, T. Pietzsch, S. Preibisch, C. Rueden, S. Saalfeld, B. Schmid, J. Y. Tinevez, D. J. White, V. Hartenstein, K. Eliceiri, P. Tomancak, A. Cardona, Fiji: An open-source platform for biological-image analysis. *Nat. Methods* **9**, 676–682 (2012).
67. J. Schindelin, C. T. Rueden, M. C. Hiner, K. W. Eliceiri, The ImageJ ecosystem: An open platform for biomedical image analysis. *Mol. Reprod. Dev.* **82**, 518–529 (2015).

Acknowledgments: We thank A. Bäumler (University of California, Davis) for providing *S.* Typhimurium mutants. **Funding:** This work was supported by NIH/National Institute of Allergy and Infectious Disease grants R01AI098078, R01AI112949, and R21AI126860. G.T.W. was also supported by Animal Models of Infectious Diseases Training Program NIH/NIAID grant T32AI060555. G.Y. was supported by a fellowship from the China Scholarship Council. J.Y.T. was supported by the NIH grant T35OD010956. L.S. was supported by a grant from the Postdoctoral Scholars Program at St. George's University. **Author contributions:** Conceived and designed the experiments: G.T.W. and R.M.T.; performed the experiments and generated mutant *S.* Typhimurium strains: G.T.W., G.Y., J.Y.T., J.L.R., B.C.E., F.F., and L.S.; analyzed the data: G.T.W. and B.P.B.; and writing: G.T.W. and R.M.T. **Competing interests:** The authors declare that they have no competing interests. **Data and materials availability:** All data needed to evaluate the conclusions in the paper are present in the paper and/or the Supplementary Materials. Additional data related to this paper may be requested from the authors.

Submitted 2 July 2020
Accepted 17 May 2021
Published 30 June 2021
10.1126/sciadv.abd6232

Citation: G. T. Walker, G. Yang, J. Y. Tsai, J. L. Rodriguez, B. C. English, F. Faber, L. Souvannaseng, B. P. Butler, R. M. Tsolis, Malaria parasite infection compromises colonization resistance to an enteric pathogen by reducing gastric acidity. *Sci. Adv.* **7**, eabd6232 (2021).